Journal of Power Sources 256 (2014) 178–182

Contents lists available at ScienceDirect

Journal of Power Sources

journal homepage: www.elsevier.com/locate/jpowsour

Short communication

Synthesis of layered cathode material $0.5Li_2MnO_3 \cdot 0.5LiMn_{1/3}Ni_{1/3}Co_{1/3}O_2$ by an improved co-precipitation method for lithium-ion battery

Zhenye Zhu*, Linwei Zhu

New Material Technology National Key Lab, School of Material Science and Engineering, Harbin Institute of Technology, Shenzhen Graduate School, Shenzhen 518055, PR China

HIGHLIGHTS

- $0.5Li_2MnO_3 \cdot 0.5LiMn_{1/3}Ni_{1/3}Co_{1/3}O_2$ is synthesized by two-step co-precipitation method.
- The initial discharge capacity of 276.7 mAh g^{-1} can be obtained at 25 mA g^{-1}.
- The capacity retention reaches to 93.06% after 50 cycles at 125 mA g^{-1}.
- Cycling stability and rate capacity have been greatly improved.

ARTICLE INFO

Article history:
Received 19 November 2013
Received in revised form
28 December 2013
Accepted 14 January 2014
Available online 25 January 2014

Keywords:
Cathode material
Li-rich
Two-step co-precipitation
Lithium-ion batteries

ABSTRACT

The layered $0.5Li_2MnO_3 \cdot 0.5LiMn_{1/3}Ni_{1/3}Co_{1/3}O_2$ lithium-rich manganese-based solid solution cathode material has been synthesized by two-step co-precipitation method. X-ray diffraction studies reveal that the as-prepared material has a typical layered structure with *R*-3*m* and *C*2/*m* space group. The surface morphology of the $[Mn_{4/6}Ni_{1/6}Co_{1/6}]CO_3$ precursor and cathode material $0.5Li_2MnO_3 \cdot 0.5LiMn_{1/3}Ni_{1/3}Co_{1/3}O_2$ have been examined using scanning electron microscopy. Electrochemical performances, including discharge capacity, cycling performance and rate capability also have been investigated. The results show that the cathode material $0.5Li_2MnO_3 \cdot 0.5LiMn_{1/3}Ni_{1/3}Co_{1/3}O_2$ prepared by two-step co-precipitation method has a good electrochemical performance, which can deliver a high initial discharge capacity of 276.70 mAh g^{-1} at the current density of 25 mA g^{-1}. When cycling at 125 mA g^{-1}, the material indicates an initial discharge capacity of 211.31 mAh g^{-1} and 196.64 mAh g^{-1} after 50 cycles, capacity retention is 93.06% and its coulombic efficiencies is greater than 98% at each charge/discharge cycling. Furthermore, the as-prepared material $0.5Li_2MnO_3 \cdot 0.5LiMn_{1/3}Ni_{1/3}Co_{1/3}O_2$ also shows an excellent rate capacity.

© 2014 Elsevier B.V. All rights reserved.

1. Introduction

Lithium-ion battery, which have been widely used for mobile electronics, is one of the most processing energy storage devices for electric vehicles (EVs) and hybrid electric vehicles (HEVs) due to its high energy storage capacity, excellent cycling stability and environmentally friendly [1,2]. In the three primary functional components of lithium-ion battery, cathode material plays a decisive role on its electrochemical properties. Since 1991, the cathode material $LiCoO_2$ was commercialized by Sony Corporation. But $LiCoO_2$ has limitations with respect to capacity, thermal stability, high cost, and chemical stability at high states of charge (above 4.3 V). Therefore, there is a strong demand to find some new alternative cathode materials to solve these problems [3–5].

Among all the reported cathode materials so far, the layered manganese-based lithium metal oxides (Li–Ni–Mn–Co) are attractive cathode materials, because of their lower cost, excellent cycling and thermal stability [6–13]. In particular, 'layered–layered' $xLi_2MnO_3 \cdot (1-x)LiMn_{1/3}Ni_{1/3}Co_{1/3}O_2$ lithium-rich manganese-based solid solution cathode materials which are comprised of two layered components, are known to deliver a discharge capacity of 200–250 mAh g^{-1} when charged to high potentials, and their capacities are almost twice than that of a conventional Li_xCoO_2 electrode [14–20]. However, 'layered–layered' $xLi_2MnO_3 \cdot (1-x)LiMn_{1/3}Ni_{1/3}Co_{1/3}O_2$ lithium-rich manganese-based solid solution cathode materials still have several performance drawbacks, such as large irreversible capacity loss (20–30%) in the first cycle, poor rate capacity performance, and poor cycling stability, especially at high current density [21–25]. Therefore, some synthesis methods

* Corresponding author. Tel.: +86 0755 26032709.
E-mail address: zhuzy@hitsz.edu.cn (Z. Zhu).

0378-7753/$ – see front matter © 2014 Elsevier B.V. All rights reserved.
http://dx.doi.org/10.1016/j.jpowsour.2014.01.068

such as co-precipitation and sol–gel method, etc. have been used to optimize their properties. So far, their cyclic stability and rate performance are still not well improved [10,12,26,27]. At present, an improved co-precipitation approach is proposed to prepare the layered manganese-based lithium metal oxides cathode materials.

In this work, we have successfully synthesized the layered lithium-rich manganese-based solid solution cathode material $0.5Li_2MnO_3 \cdot 0.5LiMn_{1/3}Ni_{1/3}Co_{1/3}O_2$ by the two-step co-precipitation method for the first time. Characterizations were carried out to examine the morphology, and crystalline structure of the composite material. Moreover, the electrochemical properties, including initial capacity, cyclic voltammetry, cycling behaviors, and rate capabilities of the cathode material $0.5Li_2MnO_3 \cdot 0.5LiMn_{1/3}Ni_{1/3}Co_{1/3}O_2$ were also investigated.

2. Experimental

2.1. Synthesis: two-step co-precipitation method

The $0.5Li_2MnO_3 \cdot 0.5LiMn_{1/3}Ni_{1/3}Co_{1/3}O_2$ cathode material was synthesized by two-step co-precipitation method. High-grade $NiSO_4 \cdot 7H_2O$ (Shanghai Aladdin, 99.9%), $CoSO_4 \cdot 7H_2O$ (Shanghai Aladdin, 99.999%) and $MnSO_4 \cdot H_2O$ (Shanghai Aladdin, 99%) were used as raw materials. Fig. 1 shows the preparation procedure of precursor $[Mn_{4/6}Ni_{1/6}Co_{1/6}]CO_3$ and cathode material $0.5Li_2MnO_3 \cdot 0.5LiMn_{1/3}Ni_{1/3}Co_{1/3}O_2$.

Firstly, a certain amount of $NiSO_4 \cdot 7H_2O$ and $CoSO_4 \cdot 7H_2O$ (3:1 molar ratio) were dissolved in distilled water and put into the reaction tank together. Then, we added the stoichiometric amount of $NaCO_3$ aqueous solution dropwise, while stirring and controlling the temperature at 50 °C, into the mixed solution. After completion of the dropwise-addition, let the reaction temperature raised to 80 °C, and then the aqueous solution containing $MnSO_4 \cdot H_2O$, $NiSO_4 \cdot 7H_2O$, and $CoSO_4 \cdot 7H_2O$ (0.8:0.05:0.15 molar ratio) were added dropwise into the continuous stirred stock solution tank containing the starting nickel-rich solution, while the required stoichiometric amounts of $NaCO_3$ aqueous solution was also added drop by drop into the reaction tank. Solution reactions were performed under a nitrogen atmosphere. The resultant slurry was aged in a sealed container at 80 °C for 12 h. Then, the $[Ni_{1/6}Co_{1/6}Mn_{4/6}]CO_3$ precipitate was isolated by vacuum filtration procedure and washed several times with distilled deionized water, and dried in air at 110 °C for 12 h. Thereafter, the obtained $[Ni_{1/6}Co_{1/6}Mn_{4/6}]CO_3$ powder was thoroughly mixed with the stoichiometrically required amount of Li_2CO_3 to prepare the targeted $0.5Li_2MnO_3 \cdot 0.5LiMn_{1/3}Ni_{1/3}Co_{1/3}O_2$ composite. Then the mixed powder was calcined in air atmosphere by two steps as follows: firstly at 500 °C for 5 h and then at 850 °C for 20 h. It was noted that the heating rate was maintained at 5 °C min^{-1}.

2.2. Structure and morphology

The morphology and particle size distribution of the synthesized material were observed by Scanning Electron Microscopy (SEM, Hitachi). Powder X-ray diffraction (XRD) patterns were performed on Rigaku RINT2000 using Cu-Kα radiation. The measurement was carried out at $2\theta = 10°–80°$, with a scan rate of 6° min^{-1}.

2.3. Electrochemical measurements

Electrochemical properties of the synthesized material were carried out by using a coin cells (type CR2025) in the voltage range of 2.0–4.8 V. The positive electrode was prepared by spreading mixture of prepared powders (80 wt%), carbon conducting additive (Super-P Li 10 wt%) and polyvinylidene fluoride (PVDF 10 wt%) dissolved in N-methyl-2-pyrrolidone (NMP) onto a smooth aluminum foil. The electrode was allowed to dry for 10 h at 120 °C in a vacuum oven. The resulting electrode film was then punched into circular discs. The negative electrode was lithium foil, and the electrolyte was 1 M $LiPF_6$ dissolved in a mixture of ethylene carbonate (EC) and dimethyl carbonate (DMC) with volume ratio 1:1. Celgard 2400 membrane was used as the separator. The current value for 1C rate was 250 mAh g^{-1}.

3. Results and discussions

3.1. Structure and morphology

Fig. 2 shows the XRD patterns of the synthesized precursor $[Mn_{4/6}Ni_{1/6}Co_{1/6}]CO_3$ and cathode material $0.5Li_2MnO_3 \cdot 0.5LiMn_{1/3}Ni_{1/3}Co_{1/3}O_2$. In Fig. 2, the diffraction peaks of precursor $[Mn_{4/6}Ni_{1/6}Co_{1/6}]CO_3$ are well consistent with $MnCO_3$ (JCPDS#83-1763), and the slight impurity might be some MnO_2 [28].

The diffraction peaks of $0.5Li_2MnO_3 \cdot 0.5LiMn_{1/3}Ni_{1/3}Co_{1/3}O_2$ are indexed by two-phase system consisting of rhombohedral $LiMO_2$ (*R*-3*m*, α-$NaFeO_2$ structure) and layered monoclinic Li_2MnO_3 (*C*2/*m*), which was consist with the previous studies [6,8,14–16]. The reflection peaks between 20° and 25° originated from the ordering of lithium ions with transition metal ions in the transition metal layers, corresponding to Li_2MnO_3 phase. As shown in Fig. 2, both the (006)/(102) and (108)/(110) doublets are clearly separated, indicating that the layered structures have good hexagonal ordering. The ratio of I(003)/I(104) is 1.423 (>1.2), which also demonstrates the formation of layered structure [29–31].

Fig. 3 describes SEM morphology of the precursor $[Mn_{4/6}Ni_{1/6}Co_{1/6}]CO_3$ and cathode material $0.5Li_2MnO_3 \cdot 0.5LiMn_{1/3}Ni_{1/3}Co_{1/3}O_2$. According to SEM morphology of the cathode material $0.5Li_2MnO_3 \cdot 0.5LiMn_{1/3}Ni_{1/3}Co_{1/3}O_2$, we found that the cathode material is composed of microspheres with the diameters of about

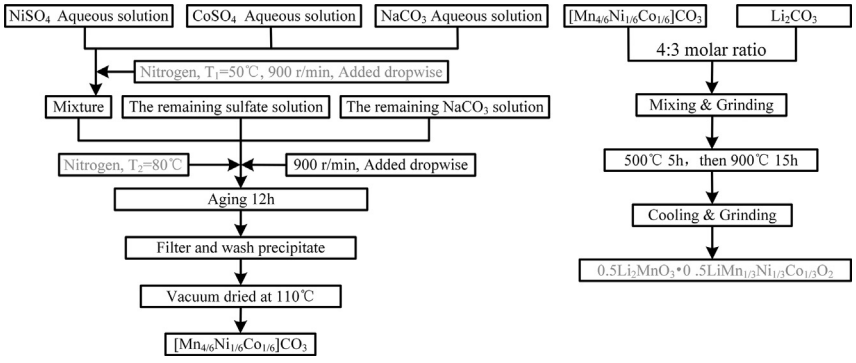

Fig. 1. Schematic diagram of the synthesis of precursor $[Mn_{4/6}Ni_{1/6}Co_{1/6}]CO_3$ and cathode material $0.5Li_2MnO_3 \cdot 0.5LiMn_{1/3}Ni_{1/3}Co_{1/3}O_2$.

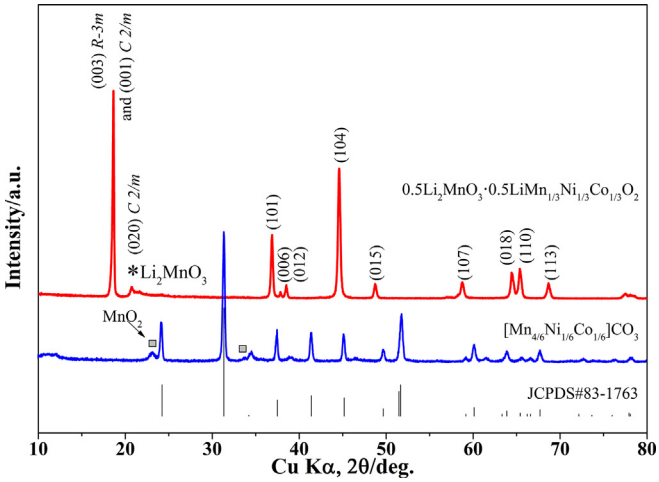

Fig. 2. XRD patterns of $[Mn_{4/6}Ni_{1/6}Co_{1/6}]CO_3$ and cathode material $0.5Li_2MnO_3\cdot0.5LiMn_{1/3}Ni_{1/3}Co_{1/3}O_2$.

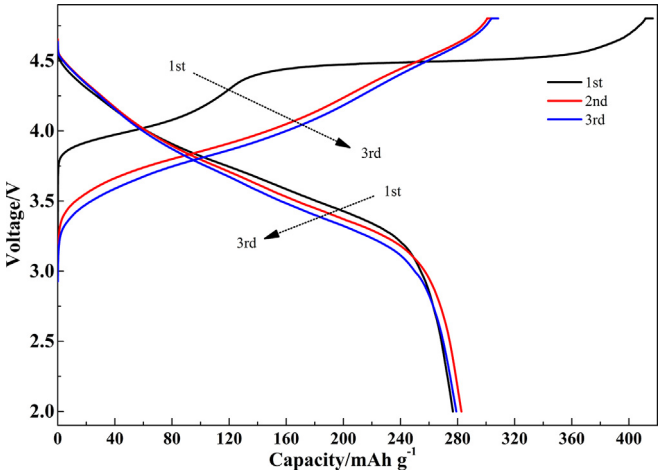

Fig. 4. Charge/discharge curves for the initial three cycles of $0.5Li_2MnO_3\cdot0.5LiMn_{1/3}Ni_{1/3}Co_{1/3}O_2$ under a current density of 25 mA g^{-1}.

5 μm, which is expected that such microspheres particles can exhibit high power performances.

3.2. Electrochemical performance

Fig. 4 exhibits the charge–discharge cycle operated at a constant current density of 25 mA g^{-1} between 2.0 and 4.8 V *vs.* Li/Li^+ at room temperature. The $0.5Li_2MnO_3\cdot0.5LiMn_{1/3}Ni_{1/3}Co_{1/3}O_2$ electrode synthesized by two-step co-precipitation method delivers an initial discharge capacity of 276.7 mAh g^{-1}, higher than that synthesized by conventional co-precipitation method. For example, Toprakci et al. [4] studied that the material can deliver an initial discharge capacity of 192 mAh g^{-1} at a current density of 20 mA g^{-1}, and Liu et al. [16] found that the material prepared by conventional co-precipitation method can deliver an initial discharge capacity of about 240 mAh g^{-1} at a current density of 20 mA g^{-1}. As indicated in Fig. 4, the material shows discharge capacity of 282.7 and 279.1 mAh g^{-1} at the second and third cycle, respectively. During the first charge, there are two plateaus located at 3.7–4.5 V and above 4.5 V. The first plateau is attributed to lithium ion extraction from $LiNi_{1/3}Co_{1/3}Mn_{1/3}O_2$ phase [13]. The second plateau is considered to be the Li_2O taking off from the layered Li_2MnO_3 structure, which results in high irreversible charge capacity of $0.5Li_2MnO_3\cdot0.5LiMn_{1/3}Ni_{1/3}Co_{1/3}O_2$ electrode [32].

To further examine the intercalation and deintercalation processes of lithium ions under different voltage limits, the cyclic voltammograms were examined. Fig. 5 presents typical cyclic voltammograms (CVs) of $0.5Li_2MnO_3\cdot0.5LiMn_{1/3}Ni_{1/3}Co_{1/3}O_2$ composite electrodes at a slow sweep rate of 0.1 mV s^{-1} in the voltage range of 2.5–4.9 V. There are two oxidation peaks at ~4.11 and ~4.64 V in the first charge process, corresponding to the oxidation of the Ni^{2+}, Co^{3+} ions and the release of oxygen, respectively. At the first discharge, there is a reduction peaks at ~3.76 V, apparently ascribed to the reduction of Ni^{4+} and Co^{4+} ions. From the second and third cycle, the CV features are significantly different from those observed in the first cycle. The strongest oxidation peak at ~4.6 V disappears and a new weak peak emerges at ~4.5 V. The two oxidation peaks at ~3.9 V and ~4.5 V should attribute to oxidation of Ni^{2+} and Co^{3+}, respectively. Meanwhile, the position of the Mn^{4+}/Mn^{3+} peak in the discharge process shifts to the left side gradually with cycles, which is associated with the structure transformation from layered to a layered-spinel intergrowth structure [8].

Fig. 6 indicates discharge capacities and corresponding coulombic efficiencies of the layered material $0.5Li_2MnO_3\cdot0.5LiMn_{1/3}Ni_{1/3}Co_{1/3}O_2$ for 50 cycles at the current density of 0.5C (125 mA g^{-1}) in a voltage range of 2.0–4.8 V. As shown in Fig. 6, we conclude that the discharge capacity at the first and 50th cycle are 211.31 and 196.64 mAh g^{-1}, respectively, and the capacity retention at the 50th cycle remains 93.06%. Compared with the study of Guo et al. [33], in which the material synthesized by combination of co-precipitation and solid state calcination method displays the discharge capacity of ~200 and ~160 mAh g^{-1} at the first and 20th cycle (cycled between 2.0 and 4.8 V at 18 mA g^{-1}), the cycling performance of the material improved significantly. Moreover, except first-cycle coulombic efficiency of 67.90%, the material shows coulombic efficiencies greater than 98% at the subsequent cycles.

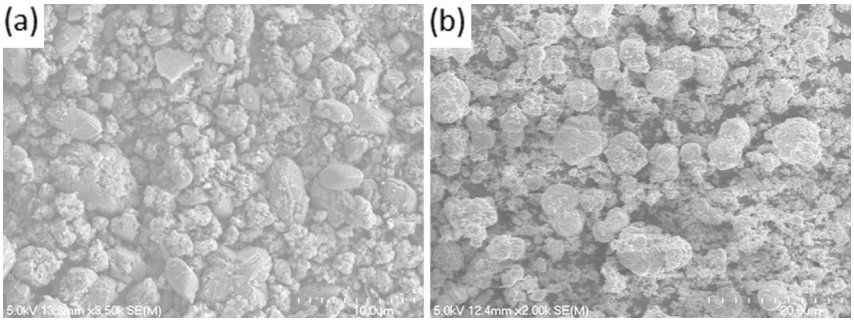

Fig. 3. SEM images of (a) $[Mn_{4/6}Ni_{1/6}Co_{1/6}]CO_3$ and (b) $0.5Li_2MnO_3\cdot0.5LiMn_{1/3}Ni_{1/3}Co_{1/3}O_2$.

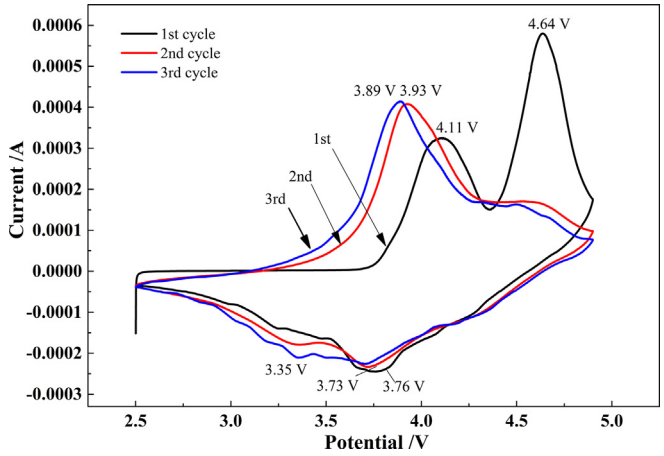

Fig. 5. Cyclic voltammograms (0.1 mV s^{-1}, 2.5–4.9 V) of $0.5Li_2MnO_3{\cdot}0.5LiMn_{1/3}Ni_{1/3}Co_{1/3}O_2$.

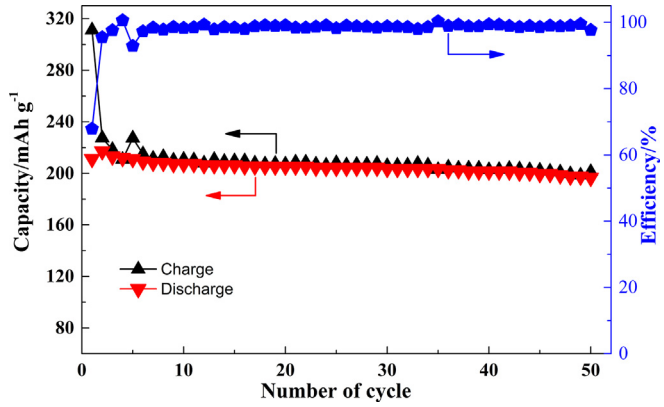

Fig. 6. Cycling performance and columbic efficiency of $0.5Li_2MnO_3{\cdot}0.5LiMn_{1/3}Ni_{1/3}Co_{1/3}O_2$ cycled at a current density of 125 mA g^{-1} (0.5C) in the voltage of 2.0–4.8 V.

Fig. 7 shows the rate capacity performance of $0.5Li_2MnO_3{\cdot}0.5LiMn_{1/3}Ni_{1/3}Co_{1/3}O_2$. The composite displays good rate capability with increasing C-rate from 0.1 to 5C. In addition, good cycling performance can be observed at each C-rate for 5 cycles. The initial discharge curves of $0.5Li_2MnO_3{\cdot}0.5LiMn_{1/3}Ni_{1/3}Co_{1/3}O_2$ at various C-rates are presented in Fig. 8. The discharge curves at different C-rates displays the same shape of Fig. 8. Under a current

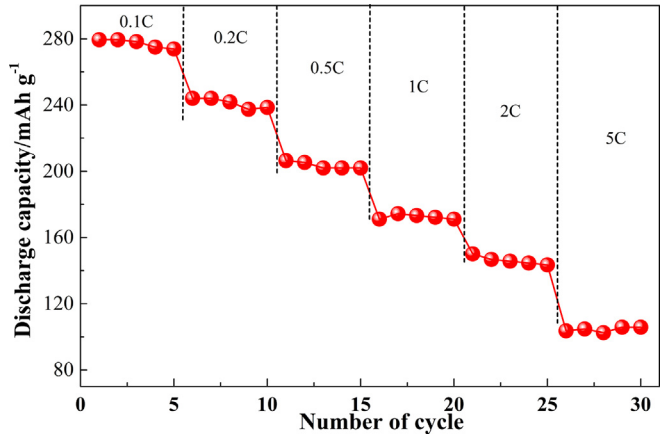

Fig. 7. Rate capability of $0.5Li_2MnO_3{\cdot}0.5LiMn_{1/3}Ni_{1/3}Co_{1/3}O_2$.

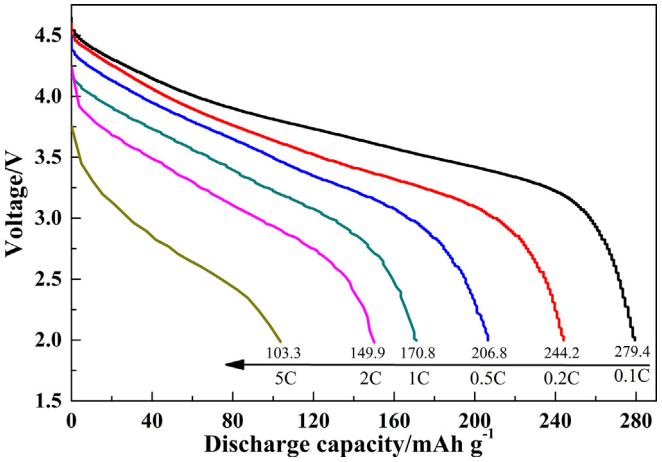

Fig. 8. Initial discharge curves of $0.5Li_2MnO_3{\cdot}0.5LiMn_{1/3}Ni_{1/3}Co_{1/3}O_2$ under different C-rates.

density of 0.1, 0.2, 0.5, 1C, 2C, and 5C, the material can deliver an initial discharge capacity of 279.4, 244.2, 206.8, 170.8, 149.9, and 103.3 mAh g^{-1}, respectively.

Based on the results discussed above, it can be concluded that the layered cathode material $0.5Li_2MnO_3{\cdot}0.5LiMn_{1/3}Ni_{1/3}Co_{1/3}O_2$ synthesized by two-step co-precipitation method shows high capacity and good rate capability, but its cycling performance still need to be improved. To address this issue and enhance the cathode performance, further work is required to modify structure and surface of cathode material.

4. Conclusions

This paper provides an excellent method (two-step co-precipitation) to fabricate the layered cathode material $0.5Li_2MnO_3{\cdot}0.5LiMn_{1/3}Ni_{1/3}Co_{1/3}O_2$ for lithium-ion batteries. Structure and morphology indicate that the as-prepared material crystallizes well with the compatible layer structure merged by Li_2MnO_3 and $LiMn_{1/3}Ni_{1/3}Co_{1/3}O_2$. The as-prepared material displays high reversible capacity and relatively good cycling stability during charge/discharge process. It can deliver a high initial discharge capacity of 276.7 mAh g^{-1} at the current density of 25 mA g^{-1}, and 211.31 mAh g^{-1} at the current density of 125 mA g^{-1}, and the discharge capacity decreases to 196.64 mAh g^{-1} after 50 cycles. The cycle performance and rate capability of the material is also relatively good.

Acknowledgments

This project was supported by Shenzhen Strategic Emerging Industry Development funds projects (No. JCYJ2013032916-1414809) and the National Natural Science Foundation of China (Nos. 11372085 and 10902029).

References

[1] M. Park, X. Zhang, M. Chung, G.B. Less, A.M. Sastry, J. Power Sources 195 (2010) 7904–7929.
[2] K.-S. Lee, S.-T. Myung, Y.-K. Sun, J. Power Sources 195 (2010) 6043–6048.
[3] A.R. Armstrong, P.G. Bruce, Nature 381 (1996) 499–500.
[4] O. Toprakci, H.A. Toprakci, L. Ying, J. Liwen, X. Leigang, H. Lee, S. Zhang, X. Zhang, J. Power Sources 241 (2013) 522–528.
[5] J.-M. Tarascon, M. Armand, Nature 414 (2001) 359–367.
[6] C. Yu, G. Li, X. Guan, J. Zheng, L. Li, T. Chen, Electrochim. Acta 81 (2012) 283–291.
[7] J.R. Croy, K.G. Gallagher, M. Balasubramanian, Z. Chen, Y. Ren, D. Kim, S.-H. Kang, D.W. Dees, M.M. Thackeray, J. Phys. Chem. C 117 (2013) 6525–6536.

[8] C.S. Johnson, N. Li, C. Lefief, J.T. Vaughey, M.M. Thackeray, Chem. Mater. 20 (2008) 6095–6106.
[9] S.-H. Kang, M. Thackeray, J. Electrochem. Soc. 155 (2008) A269–A275.
[10] M.-W. Jang, H.-G. Jung, B. Scrosati, Y.-K. Sun, J. Power Sources 220 (2012) 354–359.
[11] D. Mohanty, S. Kalnaus, R.A. Meisner, K.J. Rhodes, J. Li, E.A. Payzant, D.L. Wood III, C. Daniel, J. Power Sources 229 (2013) 239–248.
[12] D. Kim, G. Sandi, J.R. Croy, K.G. Gallagher, S.-H. Kang, E. Lee, M.D. Slater, C.S. Johnson, M.M. Thackeray, J. Electrochem. Soc. 160 (2013) A31–A38.
[13] J.-S. Kim, C.S. Johnson, J.T. Vaughey, M.M. Thackeray, S.A. Hackney, W. Yoon, C.P. Grey, Chem. Mater. 16 (2004) 1996–2006.
[14] C. Yu, H. Wang, X. Guan, J. Zheng, L. Li, J. Alloys Compd. 546 (2013) 239–245.
[15] F. Amalraj, D. Kovacheva, M. Talianker, L. Zeiri, J. Grinblat, N. Leifer, G. Goobes, B. Markovsky, D. Aurbach, J. Electrochem. Soc. 157 (2010) A1121–A1130.
[16] J. Liu, L. Chen, M. Hou, F. Wang, R. Che, Y. Xia, J. Mater. Chem. 22 (2012) 25380–25387.
[17] J. Lin, D. Mu, Y. Jin, B. Wu, Y. Ma, F. Wu, J. Power Sources 230 (2013) 76–80.
[18] J. Wang, B. Qiu, H. Cao, Y. Xia, Z. Liu, J. Power Sources 218 (2012) 128–133.
[19] M.M. Thackeray, S.-H. Kang, C.S. Johnson, J.T. Vaughey, R. Benedek, S. Hackney, J. Mater. Chem. 17 (2007) 3112–3125.
[20] J. Zheng, M. Gu, J. Xiao, P. Zuo, C. Wang, J.-G. Zhang, Nano Lett. 13 (2013) 3824–3830.
[21] S.-T. Myung, K.-S. Lee, Y.-K. Sun, H. Yashiro, J. Power Sources 196 (2011) 7039–7043.
[22] R. Santhanam, P. Jones, A. Sumana, B. Rambabu, J. Power Sources 195 (2010) 7391–7396.
[23] N. Yabuuchi, K. Yoshii, S.-T. Myung, I. Nakai, S. Komaba, J. Am. Chem. Soc. 133 (2011) 4404–4419.
[24] S. Mandal, R. Rojas, J. Amarilla, P. Calle, N. Kosova, V. Anufrienko, J. Rojo, Chem. Mater. 14 (2002) 1598–1605.
[25] S.K. Martha, J. Nanda, G.M. Veith, N.J. Dudney, J. Power Sources 199 (2012) 220–226.
[26] L. Zhao, W. Wang, A. Wang, K. Yuan, S. Chen, Y. Yang, J. Power Sources 233 (2013) 23–27.
[27] F. Amalraj, M. Talianker, B. Markovsky, D. Sharon, L. Burlaka, G. Shafir, E. Zinigrad, O. Haik, D. Aurbach, J. Lampert, J. Electrochem. Soc. 160 (2013) A324–A337.
[28] R. Alcántara, M. Jaraba, P. Lavela, J.L. Tirado, Chem. Mater. 15 (2003) 1210–1216.
[29] B. Hwang, R. Santhanam, C. Chen, J. Power Sources 114 (2003) 244–252.
[30] R. Alcántara, P. Lavela, J.L. Tirado, R. Stoyanova, E. Zhecheva, J. Electrochem. Soc. 145 (1998) 730–736.
[31] J. Dahn, U. von Sacken, C. Michal, Solid State Ionics 44 (1990) 87–97.
[32] S.J. Shi, J.P. Tu, Y.Y. Tang, Y.X. Yu, Y.Q. Zhang, X.L. Wang, C.D. Gu, J. Power Sources 228 (2013) 14–23.
[33] X.-J. Guo, Y.-X. Li, M. Zheng, J.-M. Zheng, J. Li, Z.-L. Gong, Y. Yang, J. Power Sources 184 (2008) 414–419.